GEOPHYSICAL RESEARCH LETTERS, VOL. 9, NO. 10, PAGES 1147-1150, OCTOBER 1982

VOYAGER ULTRAVIOLET STELLAR OCCULTATION MEASUREMENTS OF THE COMPOSITION AND THERMAL PROFILES OF THE SATURNIAN UPPER ATMOSPHERE

M. C. Festou and S. K. Atreya[1]
Department of Atmospheric and Oceanic Science, Space Physics Research Laboratory
The University of Michigan, Ann Arbor, Michigan 48109

Abstract. Occultation of the star δ-Scorpii by Saturn as recorded by the Voyager Ultraviolet Spectrometer yields the value of the exospheric temperature in the equatorial region to be 800 (+150, −120) K at an altitude of 1540 km above the 1-bar atmospheric pressure level; the H_2-density at 1540 km is determined to be 5 (+3.6, −1.8) x 10^9 cm^{-3}. Temperature gradient in the thermosphere is found to be 1.25 (+0.05, −0.07) K km^{-1}. Methane volume mixing ratio at 965 km above the 1-bar pressure level is determined to be 1.5 x 10^{-4}.

Introduction

The ultraviolet spectrometer (UVS) of the Voyager 2 spacecraft monitored on July 9, 1979, the occultation of the star Regulus (α-Leo) by Jupiter. From the observed absorption in the 900-1600Å wavelength range, the composition, thermal profile and eddy diffusion coefficient of the Jovian upper atmosphere were determined (Festou, *et al.*, 1981; Atreya, *et al.*, 1981). On August 25, 1981, a similar occultation experiment was conducted from the same spacecraft as light from the star Dzuba (δ-Scorpii) passed through the upper atmosphere of Saturn (Sandel, *et al.*, 1982). The analysis of the two sets of experimental data are very similar, though not entirely identical, and a detailed account of the method of data reduction and analysis as well as the characteristics of the UVS instrument are found in Festou, *et al.* (1981). Thus, only significant differences will be emphasized in the present paper.

The star δ-Sco is of the B0 spectral type and consequently bluer than α-Leo — its flux around 1000Å is ten times greater than that of α-Leo. The spectrum of δ-Sco as recorded by the UVS and reduced in the manner described by Festou *et al.* (1981) is shown in Fig. 1. No signal is measurable shortward of 911Å because of the interstellar atomic hydrogen absorption. The decrease of the signal above $\lambda \simeq 1060$Å is due to the decrease of the instrumental sensitivity. The present data were collected during the exit of the star δ-Sco from behind the disk of Saturn at a latitude of about 3.84°N and with an apparent velocity of approximately 10 km s^{-1} in a radial direction. The entry occultation data suffer from the fact that the light from the star passed through the rings before undergoing molecular absorption in the atmosphere. In the exit data, two distinct absorption regions are found: (i) below ≃ 1100Å the absorption takes place over a large range of up to 1200 km and is caused by molecular hydrogen in its Lyman and Werner band systems; and (ii) above about 1200Å, the absorption takes place over a smaller altitude range of 60 to 70 km at wavelengths below 1330Å, and over 150 to 200 km at wavelengths above 1330Å. Absorption in the 1200-1330Å range is attributed to CH_4 while that at higher wavelengths is believed to be due to an unidentified species.

The analysis of the light curves in the first region permits the determination of both the thermal and density profiles of molecular hydrogen in the thermosphere of Saturn. The analysis of one of the light curves in the second region is important for the determination of the methane mixing ratio and subsequently the value of the eddy diffusion coefficient at the homopause level. An unambiguous spectral signature of acetylene (C_2H_2), ethane (C_2H_6), or ethylene (C_2H_4) could not be discerned in the data.

[1]Send reprint requests to S. K. Atreya

Paper number 2L1329.
0094-8276/82/002L-1329$3.00

Data Reduction, Analysis, and Results

The basic data are composed of spectra of the star seen through the Saturnian atmosphere with an altitude resolution of 3.2 km and a spectral resolution of approximately 25Å. Absorption spectra are obtained by dividing those spectra by the unattenuated stellar spectrum (Fig. 1). 83 light curves that reflect the composition of the Saturnian atmosphere as a function of altitude were obtained. Since many contiguous light curves show the same time dependence, they were added together in order to increase the signal to noise ratio. Consequently, four light curves were obtained for the analysis presented here.

These correspond to: (i) channels 47-55, 939-1023Å (Fig. 2); (ii) channels 56-64, 1023-1106Å (Fig. 2); (iii) channels 80-88, 1245-1328Å (Fig. 3); and (iv) channels 89-97, 1328-1412Å (Fig. 3). Note that the spectral region around Lyman β, 1004-1041Å was not found suitable in the analysis of the Jovian stellar occultation data (Festou *et al.*, 1981) due to strong interplanetary/interstellar absorption and contribution from neighboring wavelengths on account of instrumental scattering. The δ-Sco data for Saturn have, however, been corrected for this effect, hence the inclusion of the region around Lyman β (Fig. 2). In Figures 2 through 5, the lower abscissa represents altitude above the 1-bar atmospheric pressure level while the upper abscissa shows planetocentric radii of the tangent ray points of the observations. The radii are calculated from the spacecraft trajectory information. Knowledge of the figure of Saturn along with secondary effects such as one way light travel yield a radius of 60246 ± 10 km at the 1-bar level for the δ-Sco exit occultation geometry. Subtraction of this value from the radii (upper abscissa) yields altitude above the 1-bar level (lower abscissa). The significance of "Δz" in the lower abscissa scale is that it is the height above the 1-bar level of the zero of the "experimental altitude scale"; the latter being the level at which 100% absorption (i.e. zero counts) in the short wavelength channels (here, channels 47-65) is recorded. Defining altitudes in this manner facilitates comparison of raw data and their analyses with a similar exercise for Jupiter (Festou, *et al.*, 1981) for which trajectory information was not known nearly as well as in the case of Saturn. The zero of the experimental altitude scale occurred at $23^h45^m00^s$, day 237 at a radius of 61180 km, 934 km (Δz) above the 1-bar level. The characteristics of the above mentioned data set are discussed below.

(i) *Wavelengths below ≃ 1100Å:* On examining Fig. 2, we find that for altitudes above (Δz + 60) km, and wavelengths below approximately 1100Å, the absorption characteristics of molecular hydrogen as shown in the theoretical Fig. 6 of Festou *et al.* (1981) are seen. The maximum altitude range over which absorption is seen to occur corresponds to wavelengths around 1000Å. Below this wavelength and in the (Δz + 100) to (Δz + 300) km altitude range, the absorption is found to be comparatively lower than in the deepest part of the Jovian thermosphere where absorption was detected (Festou *et al.*, 1981). If the temperatures were in the 200-400K range as on Jupiter in the corresponding altitude range,it is implied then that the total column density of the absorbing molecules is lower as compared to Jupiter's. Between 1000Å and 1100Å, a measurable absorption is observed over a range of more than 1000 km which indicates a higher average temperature in that region of absorption compared to Jupiter. Finally, above 1100Å no significant H_2-band absorption is observed for altitudes higher than (Δz + 60) km (as was the case for Jupiter, Festou *et al.*, 1981) which implies that either the total column density or the temperature is small, even in the case of the lines of sight penetrating deeper in the Saturnian atmosphere.

(ii) *Wavelengths above ≃ 1200Å:* The region between 1180 and 1240Å cannot be used because of the strong contamination by the interplanetary Lyman-alpha line. Above 1245Å, the absorption

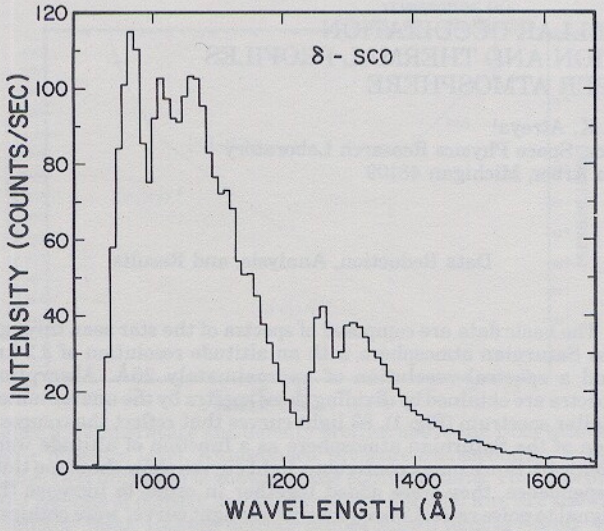

Figure 1. Unattenuated spectrum of star δ-Sco as seen by Voyager UVS. The effective spectral resolution is approximately 25Å. Background has been removed and the various instrumental corrections applied.

occurs in the range $(\Delta z + 0)$ to $(\Delta z + 60)$ km if $1245\text{Å} \lesssim \lambda \lesssim 1328\text{Å}$ (Fig. 3a), and from $(\Delta z + 0)$ to $(\Delta z + 200)$ km for $\lambda \gtrsim 1328\text{Å}$ (Fig. 3b). Tentatively, these absorptions are attributed to the hydrocarbons. Shortward of $\lambda \simeq 1100\text{Å}$, hydrocarbons may contribute to the observed absorption below $(\Delta z + 60)$ km.

The absorption in molecular hydrogen is examined first. The absorptions shown in Fig. 2 (smooth curves) were interpreted using the theoretical absorption model described by Festou *et al.* (1981) for Jupiter. The absorption characteristics of the two planets were somewhat different and required different techniques of analysis. In the case of Jupiter, the column densities in the deepest parts of the thermosphere were first determined and the complete light curves were interpreted by assuming an atmospheric temperature profile while the density was known at the bottom of the thermosphere. In the case of Saturn, the absorption in the highest

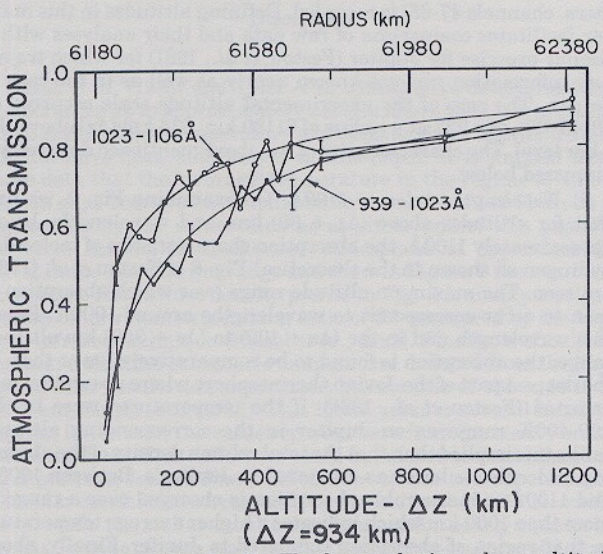

Figure 2. Absorption by H_2. The lower abscissa shows altitudes above the 1-bar pressure level while the upper abscissa gives corresponding planetocentric radii of the tangent ray points. The height resolution in this figure is 32 km, except for points above $(\Delta z + 500)$ km which have been obtained by averaging 40 consecutive spectra recorded over a 128 km height range. The continuous lines are the absorption curves which are used to derive the temperature and density profiles of H_2.

layers of the atmosphere contributes significantly to the observed absorption in the deepest parts and the technique used for Jupiter cannot be employed. Fortunately, the absorption above about $(\Delta z + 600)$ to $(\Delta z + 700)$ km can be reproduced in the 939-1106Å interval by assuming that the temperature is constant, thus effects of both temperature and density can be separated. The exospheric temperature on Saturn is reached around $(\Delta z + 600)$ to $(\Delta z + 700)$ km range. Consequently, the density can be determined unambiguously at the top of the atmosphere and complete light curves are then analyzed by working the calculations downward. Figures 4a and 4b illustrate these calculations. Each theoretical curve corresponds to a different column density-temperature combination. The best simultaneous fit to the data (see Fig. 4c) requires a temperature of 800 (+150, −120) K and an H_2 density of 5.0 (+3.6, −1.8) x 10^9 cm^{-3} at $(\Delta z + 600)$ km.

As seen in Fig. 4c, the assumption of a constant temperature in the region below $(\Delta z + 600)$ km does not hold and a decrease in the temperature with depth is the only solution for increasing the absorption. Transmission in an H_2 atmosphere was then calculated assuming a linear decrease in temperature beginning with 800 K at the $(\Delta z + 600)$ km level; the results of the calculations are shown in Fig. 5. Absorptions were computed down to the $(\Delta z + 60)$ km level or when a 140 K temperature was reached, whichever came first. No satisfactory fit with the 1023-1106Å light curve could be achieved in the $(\Delta z + 100)$ to $(\Delta z + 600)$ km altitude range. There is an indication that the absorption in the 1023-1106Å wavelength interval might be somewhat overestimated at high altitudes, consequently we chose the 939-1023Å light curve for determining the temperature gradient below $(\Delta z + 600)$ km. If the 939-1023Å light curve alone is used to determine the exospheric temperature, a value of 800 (+120, −100) K is reached at $(\Delta z + 600)$ km. The best fit to the data was found with a thermal gradient of 1.25 (+0.05, −0.07) K km^{-1}. Thus, a temperature of 140 (+35, −25) K is reached at approximately $(\Delta z + 72)$ km. Temperatures substantially below this value do not produce the observed transmission characteristics. Note also that the calculated absorption in the $(\Delta z + 60)$ to $(\Delta z + 100)$ km altitude range for the 1023-1106Å light

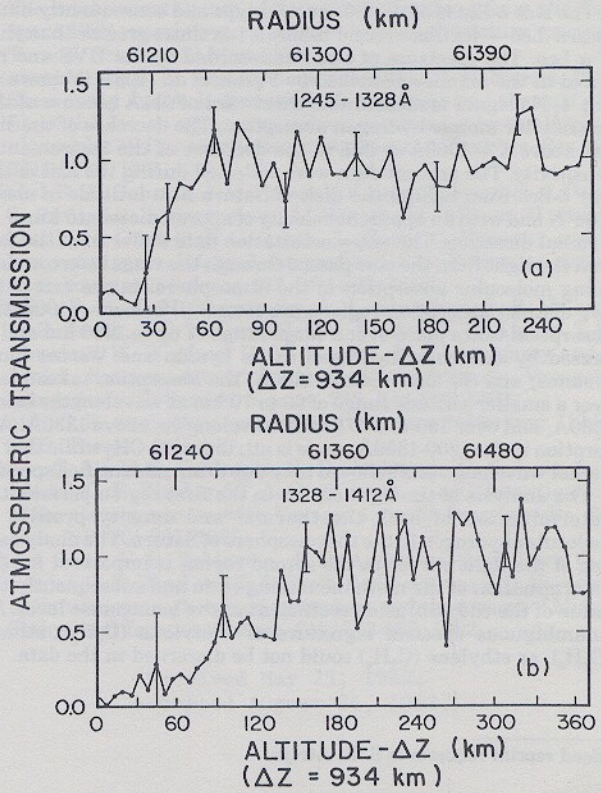

Figure 3. Absorption by the hydrocarbons: Fig. 3a, the absorption is attributed to CH_4; Fig. 3b, absorption due to an unidentified species, alone or in mixture with the hydrocarbons. Altitude scale is same as in Fig. 2.

curve is approximately right, and that the underestimation of the absorption for higher altitudes never exceeds 10%. This discrepancy could have been the result of poorly known band absorptions.

Next, the wavelength region beyond 1245Å is investigated. Contrary to the case of Jupiter, no sudden increase of the absorption, i.e. a "knife edge," was observed at a given wavelength. The various light curves for $\lambda \geq 1245$Å were grouped into two average light curves shown in Fig. 3 because the two series showed the same time dependence. From Fig. 3a, an average scale height of about 10 to 15 km is found. However, this value is not too meaningful since the scale height could be rapidly changing over the small altitude interval over which absorption is observed. From Fig. 3b, an average scale height of approximately 45 km is determined; this value is slightly below the H_2-scale height for this altitude.

If we assume that the only potential absorbers are methane (CH_4), ethane (C_2H_6), acetylene (C_2H_2) and ethylene (C_2H_4), the only acceptable candidate for producing the absorption shown in Fig. 3a is methane (see the absorption cross sections in Festou *et al.*, 1981). In the 1245-1328Å spectral range all individual light curves show nearly identical absorption features, i.e. a given optical depth always occurs at the same altitude irrespective of the wavelength range. Since the absorption cross sections of both C_2H_2 and C_2H_4 vary greatly in this wavelength interval, they cannot be responsible for the observed absorption. C_2H_6 is not acceptable as an absorber in the 1245-1328Å range either since it would produce more than observed absorption around (Δz + 50) km at shorter wavelengths. Finally, none of the four hydrocarbon absorbers (CH_4, C_2H_2, C_2H_4, and C_2H_6) have the appropriate variation in their absorption cross sections above 1328Å to produce the absorption characteristics shown in the 1328-1412Å interval, Fig. 3b. In the 1328-1412Å range data absorption begins at higher altitudes than in the previous range (1245-1328Å) and within this wavelength interval the absorption extends deeper and deeper as the wavelength of absorption increases. This phenomenon could be interpreted as being indicative of a decrease in the absorption cross section with increasing wavelength. It is not possible to reconcile the observed transmission characteristics of these two wavelength ranges from a choice of the hydrocarbons we have discussed. We believe that the absorption in the wavelength region longward of 1328Å is caused by some as yet unidentified absorber/s whose absorption cross section is greater above 1330 ± 10Å than below it. The possibility of a high altitude haze cannot be entirely ruled out.

As argued above, the absorption of Fig. 3a appears to have been produced by CH_4. One can, therefore, calculate various CH_4 atmospheric profiles by assuming that the CH_4 scale height varies linearly with increasing altitude from a mixed atmospheric scale height of approximately 61 km (corresponding to a temperature of 140 K) down to 0 km at some higher altitude. For each assumed rate of increase of the scale height, the observed amount of absorption was found to occur at a certain altitude where the scale height

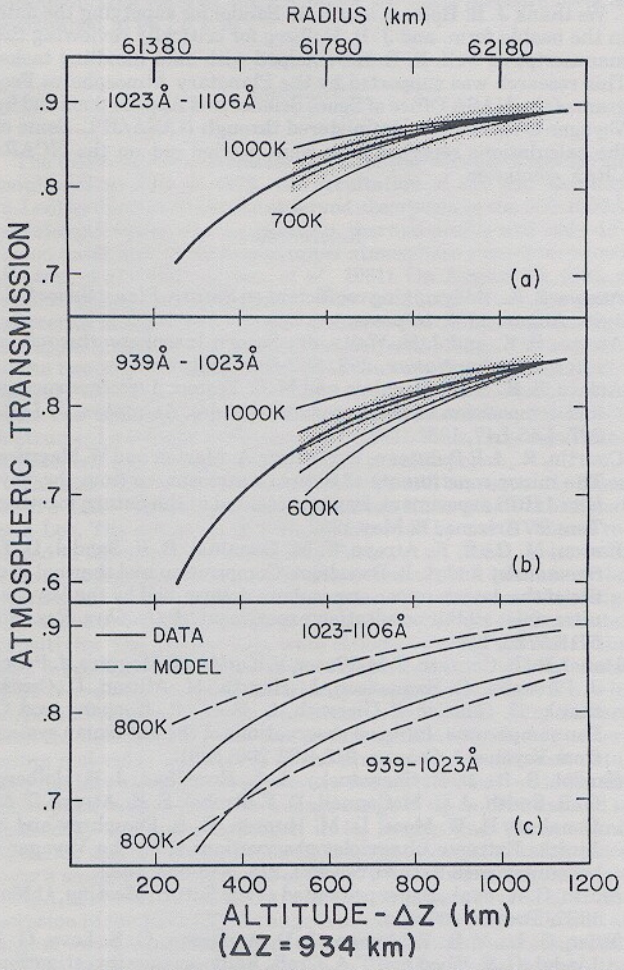

Figure 4. Measured (heavy lines, from Fig. 2) and calculated transmissions for 600K, 700K, 800K, 900K, and 1000K temperatures in the upper atmosphere of Saturn. The shaded areas in Figures 4a and 4b represent the statistical uncertainty in the data. Above about (Δz + 600) km, a constant temperature of 800 K produces the observed atmospheric transmission. The observed transmissions in Figs. 4a and 4b are reproduced by varying both the column density and the temperature in the model — the label in these figures only gives the temperature. The column densities at corresponding temperatures are not the same in Figs. 4a and 4b. Column densities are adjusted independently to produce the observed transmission at (Δz + 1100) km. When 'both' temperature and column density are chosen the best simultaneous fit to the two experimental curves is obtained, Fig. 4c. In Fig. 4c, it can be noticed that the absorption is slightly overestimated in the 939-1023Å range and slightly underestimated in the 1023-1106Å range. Altitude scale is same as in Fig. 2.

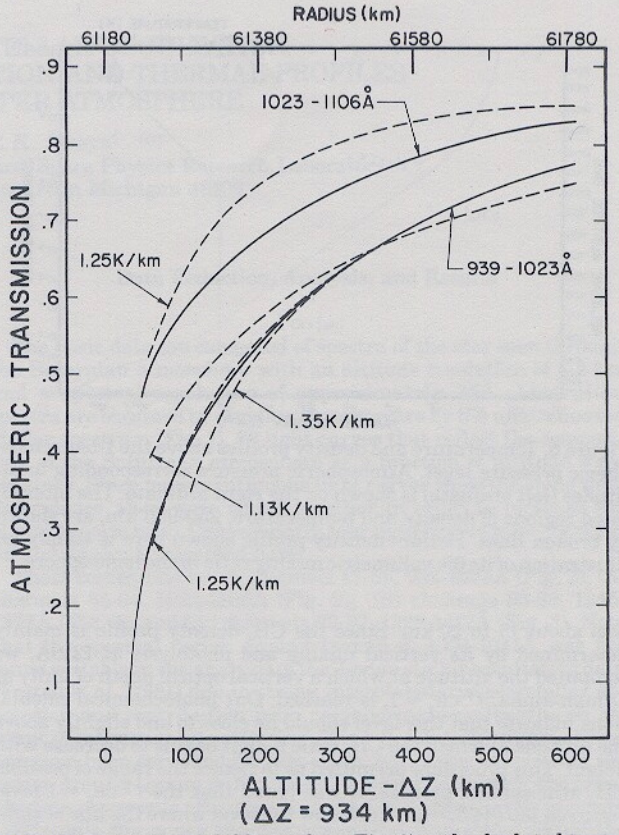

Figure 5. Measured (solid lines, from Fig. 2) and calculated transmission in H_2 in (Δz + 60) to (Δz + 600) km range. From the light curve 939-1023Å it is determined that the temperature increases linearly with altitude between (Δz + 72) km and (Δz + 600) km, varying from 140 K to 800 K with a gradient of approximately 1.25 K km^{-1}. Altitude scale is same as in Figure 2.

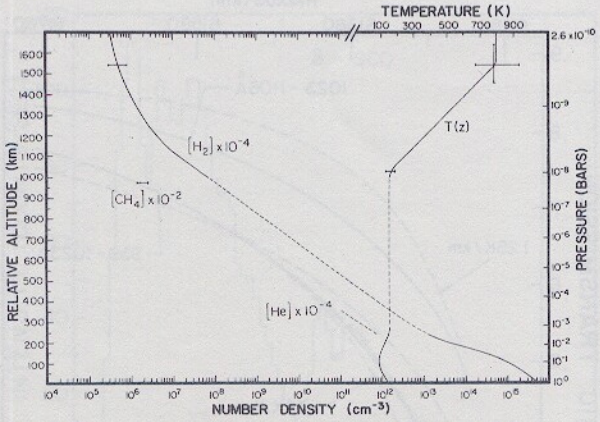

Figure 6. Temperature and density profiles above the 1-bar atmospheric pressure level. Atmospheric pressure corresponding to altitudes (left ordinate) is shown on the right ordinate. The interpolated regions of density and temperature, 250-950 km, are shown by broken lines. Helium density profile shown here is simply an illustration of its 6% volumetric mixing ratio in the homosphere.

was about 15 to 20 km. Since the CH_4-density profile is mainly determined by its vertical mixing and photolysis at 1216Å, we computed the altitude at which a vertical optical depth of unity at Lyman-alpha, $\tau^{\uparrow}_{CH_4} = 1$, is reached. Our photochemical calculations indicate that this level should lie close to and slightly above the altitude at which the CH_4 scale height begins to decrease with height. This procedure permitted us to reduce the range of possible CH_4 atmospheric profiles. It was found that the $\tau^{\uparrow}_{CH_4} = 1$ level occurred 160 (+25, −40) km below the level where the line of sight optical depth in the 1245-1328Å range is 0.5 in Fig. 3a; the latter being at ($\Delta z + 32$) km. The CH_4-density at ($\Delta z + 32$) km is found to be 1.9 (+0.9, −0.3) x 10^8 cm^{-3}; the corresponding H_2-density at this altitude is 1.2 x 10^{12} cm^{-3} giving $CH_4/H_2 = 1.5 \times 10^{-4}$ at this altitude. The H_2-density at the $\tau^{\uparrow}_{CH_4} = 1$ level is then calculated to be 1.6 (+0.9, −0.7) x 10^{13} cm^{-3}. The mixing ratio of methane in the troposphere may be as high as 1.85 (+1.2, −0.5) x 10^{-3} according to Courtin *et al.* (1982). The depletion of methane mixing ratio in the upper atmosphere is a reflection of its transport and photolysis.

Discussion

Hanel *et al.* (1981) and Tyler *et al.* (1981) have determined the temperature up to approximately 250 km above the 1-bar pressure level. Atmospheric temperature and density above approximately 950 km have been determined in this paper. It is implied from these data that the 'average' temperature in the regime of 'information gap,' 250-950 km, should be on the order of 142 K which is approximately the same value as at either end of this gap. We therefore assume an isothermal atmosphere at approximately 140 K in the 250-950 km range and show in Figure 6 the results of this paper. The helium density profile in Fig. 6 is simply an illustration of its volumetric mixing ratio of 6% measured by the Voyager infrared technique (Hanel *et al.*, 1981). Finally, it should be remarked that the exospheric temperature deduced from the Voyager 2 solar occultation experiment has a value of 485 ± 50 K at 2800 km, Smith *et al.*(1982). This latter value is several hundred degrees lower than the value reported here from the stellar occultation analysis. This difference could be related to the latitudinal (and perhaps, longitudinal) differences of the two experiments. The solar occultation corresponds to the mid latitude (36°N) conditions, while the stellar occultation data are for nearly equatorial region. Topside plasma scale height (hence temperature) of Saturn at high latitudes is also nearly one-half of the value measured at mid latitudes (Tyler *et al.*, 1982). Moreover the Voyager 2 mid latitude plasma temperatures are calculated to be 565 K at 2800 km (ingress, 36.5°N) and 617 K at 2500 km (egress, 31°S) if H^+ is the topside ion at those heights. The ionospheric structure in this range is controlled by diffusion rather than photochemical equilibrium. Thus, the average mid latitude plasma temperature is above 590 K. This value of plasma temperature is expected to overlap the statistical range of the neutral exospheric temperature reported in this paper, once statistical uncertainties in the radio occultation data have been accounted for. The major ion may not be H^+, however, but H_2^+ or H_3^+ as suggested by Atreya and Waite (1981), resulting in an even higher average plasma temperature than 590 K based on H^+.

Acknowledgment

We thank J. B. Holberg and B. R. Sandel for supplying the data in the usable form, and J. B. Holberg for critically reviewing the manuscript as well. R. B. Kerr helped with data handling tasks. This research was supported by the Planetary Atmospheres Program of the NASA Office of Space Science and Applications and by Voyager UVS Project administered through NASA/JPL. Some of the calculations reported here were carried out on the NCAR/CRAY computer.

References

Atreya, S. K., Eddy mixing coefficient on Saturn, *Planet Space Sci., 30,* August 1982, in press.

Atreya, S. K. and J. H. Waite, Jr., Saturn Inosphere: theoretical interpretation, *Nature, 292,* 682-683, 1981.

Atreya, S. K., T. M. Donahue and M. C. Festou, Jupiter: structure and composition of the upper atmosphere, *Astrophys. J. Lett., 247,* L43-L47, 1981.

Courtin, R., J. P. Balutean, D. Gautier, A. Marten and W. Maguire, The minor constituents of Saturn's atmosphere from the Voyager 1 IRIS experiment. Paper presented at the Saturn meeting, Tucson, Arizona, 12 May 1982.

Festou, M. C., S. K. Atreya, T. M. Donahue, B. R. Sandel, D. E. Shemansky and A. L. Broadfoot, Composition and thermal profile of the Jovian upper atmosphere determined by the Voyager ultraviolet stellar occultation experiment, *J. Geophys. Res., 86,* 5715-5725, 1981.

Hanel, R., B. Conrath, F. M. Flaser, V. Kunde, W. Maguire, J. Pearl, J. Pirraglia, R. Samuelson, L. Herath, M. Allison, D. Cruikshank, D. Gautier, P. Gierasch, L. Horn, R. Koppany and C. Ponnamperuma, Infrared observations of the Saturnian system from Voyager 1, *Science, 212,* 192-200, 1981.

Sandel, B. R., D. E. Shemansky, A. L. Broadfoot, J. B. Holberg, G. R. Smith, J. C. McConnell, D. F. Strobel, S. K. Atreya, T. M. Donahue, H. W. Moos, D. M. Hunten, R. B. Pomphrey and S. Linick, Extreme ultraviolet observations from the Voyager 2 encounter with Saturn, *Science, 215,* 548-553, 1982.

Smith, G. R., et al., Paper presented at the Saturn Meeting, 11 May 1982, Tucson, Arizona.

Tyler, G. L., V. R. Eshleman, J. D. Anderson, G. S. Levy, G. F. Lindal, G. E. Wood and T. A. Croft, Radio science investigations of the Saturn system with Voyager 1: preliminary results, *Science, 212,* 201-205, 1981.

Tyler, G. L., V. R. Eshleman, J. D. Anderson, G. S. Levy, G. F. Lindal, G. E. Wood and T. A. Croft, Radio science with Voyager 2 at Saturn: atmosphere and ionosphere and the masses of Mimas, Tethys and Iapetus, *Science, 215,* 553-557, 1982.

(Received May 25, 1982;
accepted August 24, 1982.)